

*copy 3*  
667

NAVY DEPARTMENT  
THE DAVID W. TAYLOR MODEL BASIN  
Washington 7, D.C.



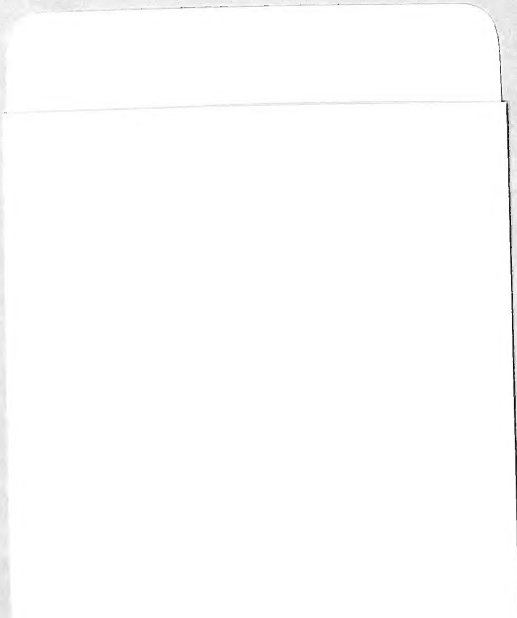
RESISTANCE AND STABILITY TESTS OF THE  
WOODS HOLE OCEANOGRAPHIC INSTITUTION  
CURRENT-INDICATOR BUOYS

BY R.A. EBNER

NOVEMBER 1948

REPORT 667

20  
1  
D3  
10-667



MBL/WHOI  
0 0301 0032445 0

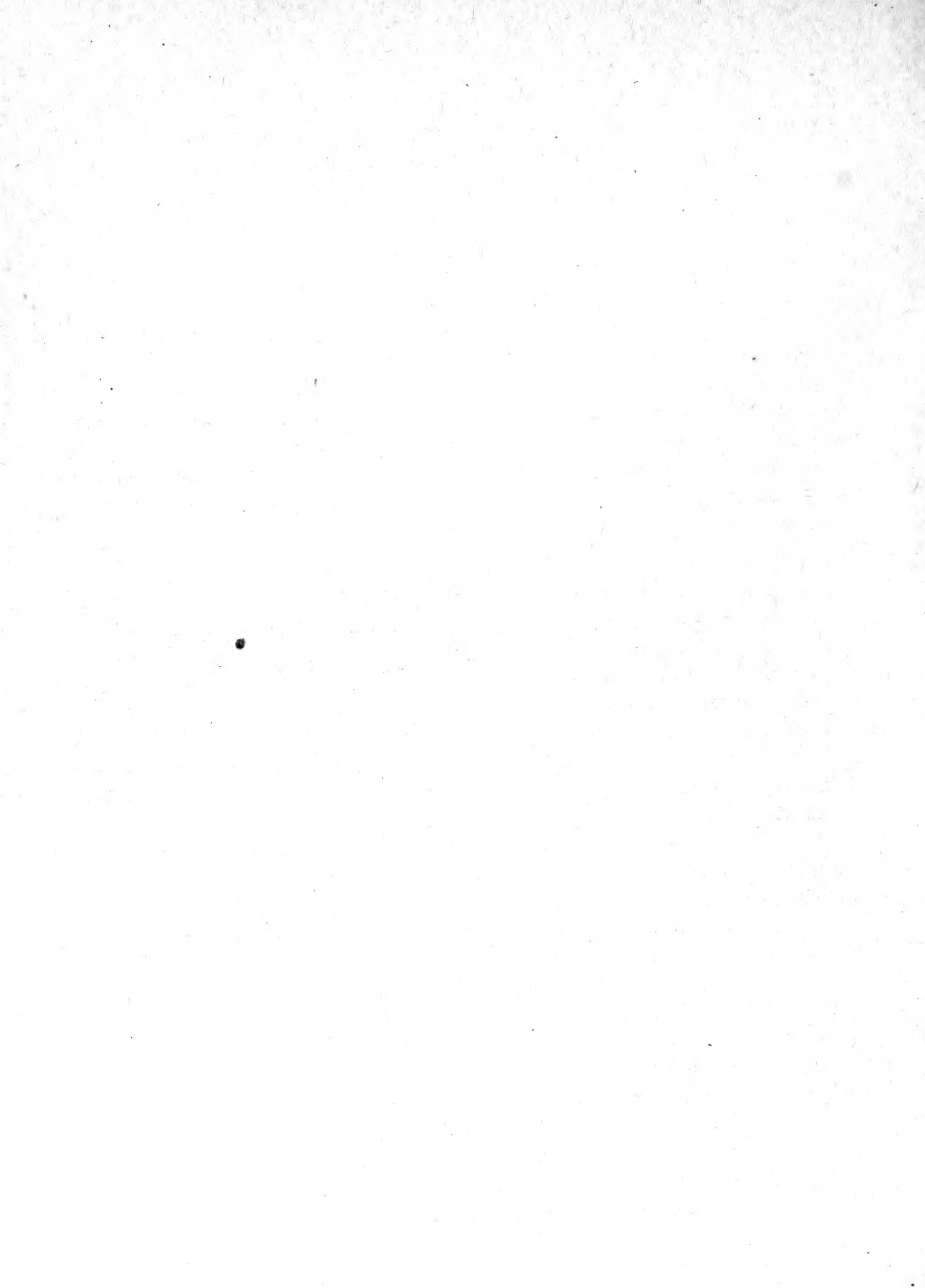


DISTRIBUTION

Initial distribution of copies of this report:

3 copies to Bureau of Ships, Project Records, Code 362.

4 copies to Woods Hole Oceanographic Institution.



RESISTANCE AND STABILITY TESTS OF THE WOODS HOLE OCEANOGRAPHIC  
INSTITUTION CURRENT-INDICATOR BUOYS

by

R.A. Ebner

ABSTRACT

The Woods Hole Oceanographic Institution has developed an instrument which in principle uses the drag of a buoy to measure current velocities. At their request the David Taylor Model Basin measured the drag of 1/3-scale models of three proposed forms for the buoy and a full-scale model of one of these forms to determine which of the forms was best suited to their purpose. The full-scale model was also tested for stability. From the tests conducted Buoy 1 was found to have the most satisfactory performance.

INTRODUCTION

At a conference held at the David Taylor Model Basin (1),\* representatives from the Woods Hole Oceanographic Institution explained a proposed device for obtaining measurements of the vertical distribution of velocity in ocean currents in water up to 200 feet deep. A system for determining this distribution was proposed. A buoy which was attached to an anchor by means of a mooring line was to be released from the ocean bottom. As the buoy slowly ascended to the surface the angle of the mooring line at the buoy was determined by the resultant direction of the weight, buoyancy, and drag forces acting on the buoy. A recording pendulum for indicating the angles which the cable assumed at various depths was to be attached directly under the buoy on the mooring cable; see Figure 1. From the angles obtained, the drag of the buoy could be computed. Hence, if the drag of the buoy was known as a function of the current velocity, the recorded angles would be made a direct measure of the velocity of the current.

It was requested that the Taylor Model Basin make resistance tests of three 1/3-scale model buoys and one full-scale model. The models were supplied by the Woods Hole Oceanographic Institution. It was also requested that tests be made to determine whether the presence of various towing bails attached to the buoys had an appreciable effect on the drag, and that a test be made to observe the stability of the full-scale model when it was towed from an underwater towpoint, simulating actual moored conditions.

---

\* Numbers in parentheses indicate references at the end of this report.

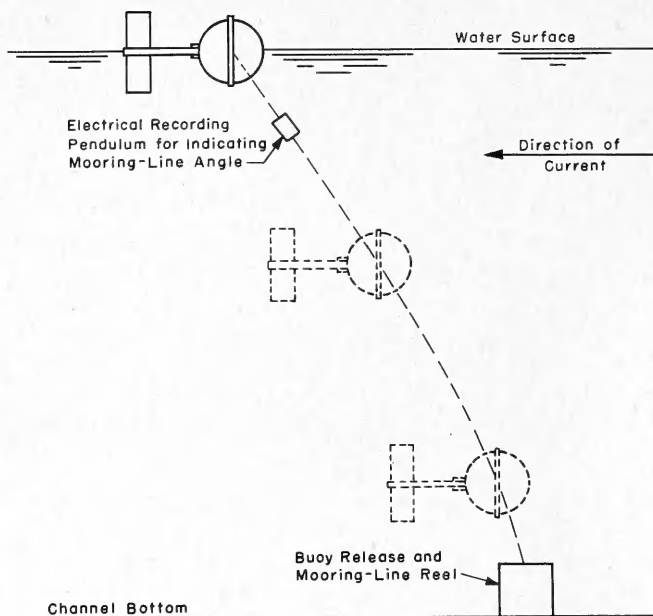


Figure 1 - Path of Current-Indicator Buoy As the Buoy Rises to the Surface After Being Released from the Bottom of the Channel

#### DESCRIPTION OF THE MODELS

Three different  $1/3$ -scale models and one full-scale model were tested for resistance in the deep-water basin of the Model Basin. The construction of the models is as follows:

The  $1/3$ -scale model of Buoy 1 is a sphere  $5 \frac{1}{3}$  inches in diameter, with a projecting ring 6 inches in outside diameter around the vertical transverse equator. When the buoy was towed the ring was normal to the direction of motion. Protruding  $1 \frac{1}{2}$  inches from the front of the sphere, forward of the ring, was a pin  $1/32$  inch in diameter, simulating the mooring line; see Figure 2. Provision was made for the pin to be placed at 10, 20, or 30 degrees from a vertical plane through the center of the sphere.

The  $1/3$ -scale model of Buoy 2 is a sphere  $5 \frac{1}{3}$  inches in diameter with a projecting ring 6 inches in outside diameter. This buoy was fitted with a bail for mooring, which necessitated placing the ring aft of the vertical transverse equator; see Figure 3.

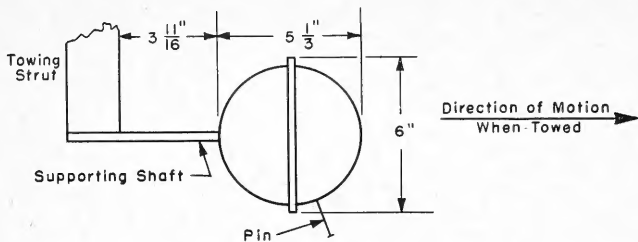


Figure 2 - Sketch of 1/3-Scale Model of Buoy 1

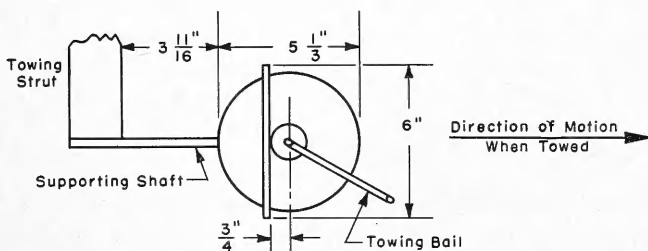


Figure 3 - Sketch of 1/3-Scale Model of Buoy 2

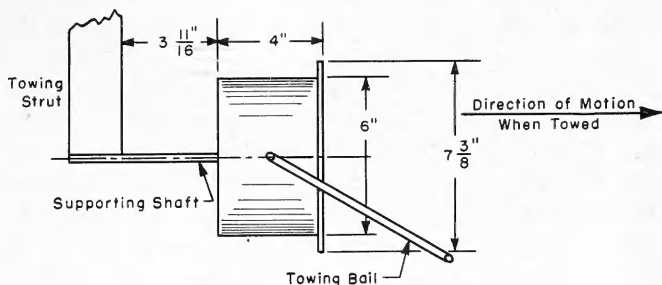


Figure 4 - Sketch of 1/3-Scale Model of Buoy 3

The 1/3-scale model of Buoy 3 is a short cylinder 6 inches in diameter with a disk  $7 \frac{3}{8}$  inches in diameter fastened on the forward end. The direction of motion on towing was along the axis of the cylinder. This model is shown in Figure 4.

The full-scale model of Buoy 1 is a 16-inch laminated wooden sphere with a projecting ring 18 inches in outside diameter around the vertical transverse equator. This sphere was mounted on one end of a  $1 \frac{1}{2}$ -inch rod and four plastic fins were mounted at the other. These fins were 24 inches

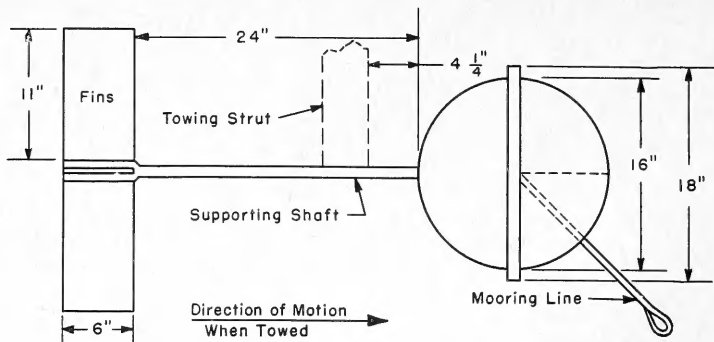


Figure 5 - Sketch of Full-Scale Model of Buoy 1

aft of the sphere and were 6 inches wide,  $1/16$  inch thick, and had a span of 24 inches. The lower forward quadrant of the vertical longitudinal plane of the sphere was slotted to permit the passage of the mooring line to the center of the sphere. Figure 5 shows the general arrangement of this buoy.

After the sphere had been immersed during several tests, separation occurred between laminations and the layers became displaced relative to each other, which produced a corrugated effect with irregularities as great as  $1/2$  inch. This necessitated the construction of another full-scale model at the Model Basin to complete the required tests.

Photographs of the models are shown in Figures 6, 7, 8, 9, and 10.



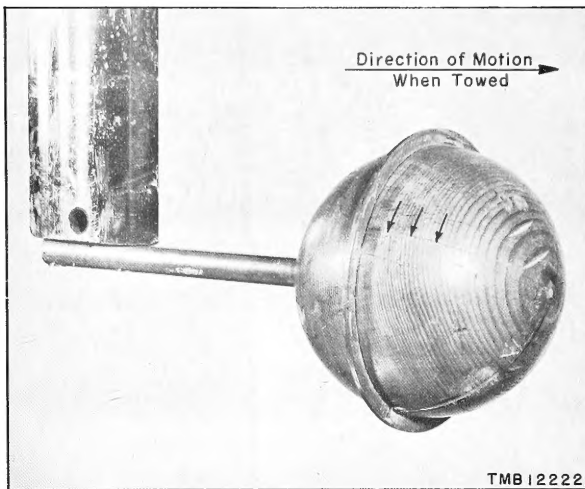


Figure 6 - 1/3-Scale Model of Buoy 1

The buoy is shown fastened to the towing strut in position for drag tests. Arrows on the buoy point to holes which receive steel pins used to simulate the mooring line of the full-scale model.

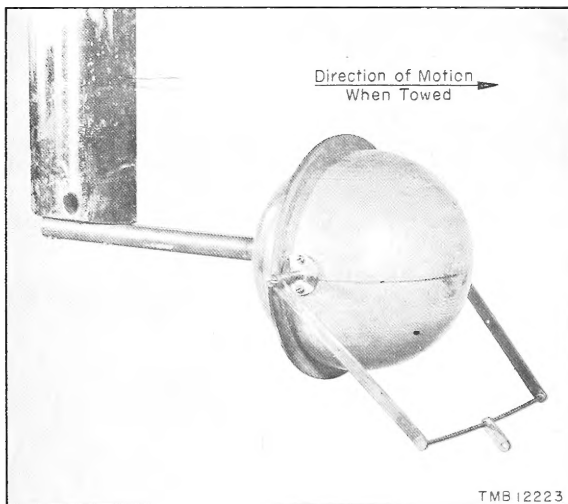


Figure 7 - 1/3-Scale Model of Buoy 2

The buoy is anchored to the end of the towing strut in the towing position. The figure shows clearly the towing bail arrangement used.

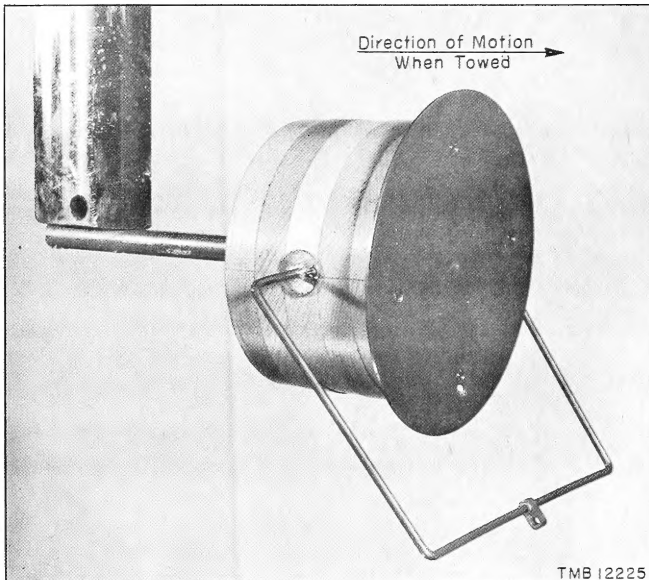


Figure 8 - 1/3-Scale Model of Buoy 3

The model with the towing bail attached is fastened to the towing strut. Excessive vibration was encountered while the buoy was being towed in this position.

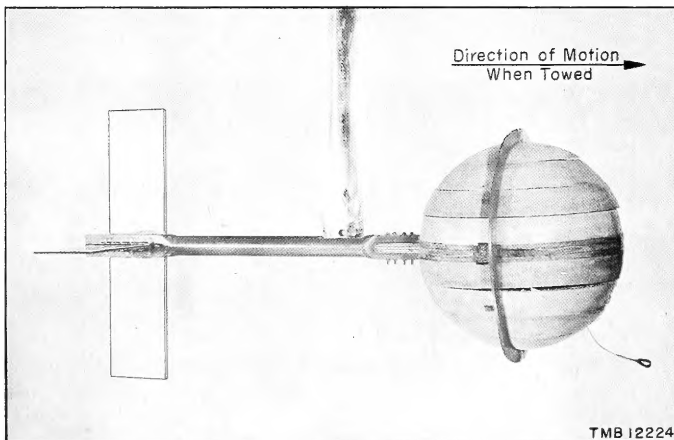


Figure 9 - Full-Scale Model of Buoy 1

The buoy is shown fastened to the end of the towing strut. Separation of the laminations is clearly shown. The wire cable extends to a pivot shaft at the center of the sphere and serves as the towing bridle for the buoy.

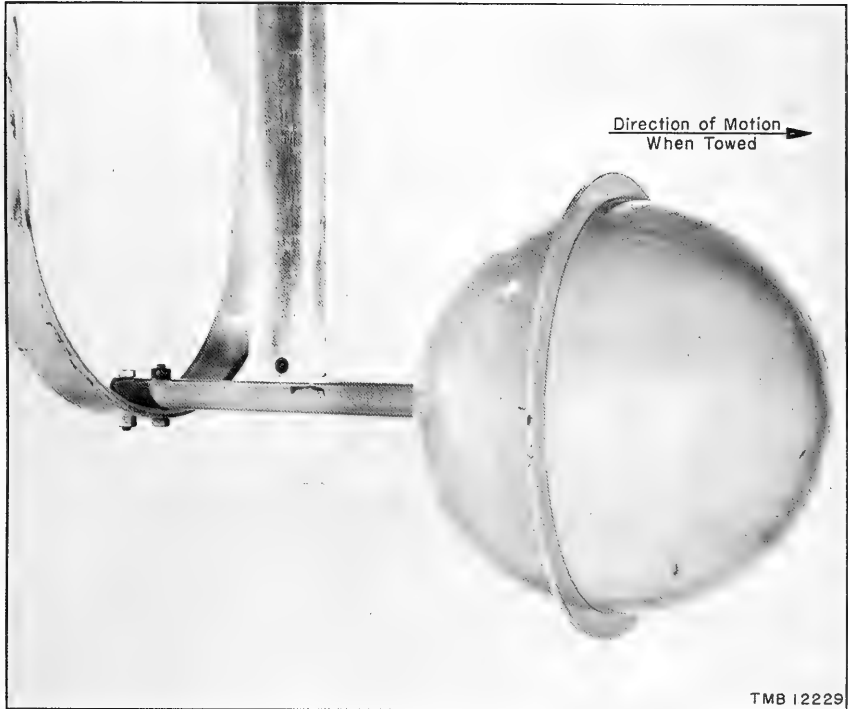


Figure 10 - Full-Scale Model of Buoy 1

This buoy was built after separation of the laminations of the Woods Hole buoy made further tests on that buoy impossible.

### TEST PROCEDURE

To measure the resistance, the buoy to be tested was fastened to the end of a towing strut which was submerged to a depth of  $34 \frac{5}{8}$  inches. The other end of the strut was clamped to the towing beam of the drag dynamometer of the towing carriage, as is shown in Figure 11. The strut was a standard towing strut for submerged bodies (2) of ogival section with a chord length of 4 inches and a thickness of 1 inch.

The  $\frac{1}{3}$ -scale model of Buoy 1 was tested at speeds between 0.20 and 13 knots for various positions of the pin simulating the mooring line.

The  $\frac{1}{3}$ -scale models of Buoys 2 and 3 were tested with and without the towing balls at speeds from 1 to 9 knots. The towing balls were mounted on the models 45 degrees below the horizontal axis of the buoy.

The full-scale model of Buoy 1 was tested for drag at speeds from 0.50 to 3.50 knots. The model was also tested for towing stability by towing a 200-pound weight from the towing carriage 18 feet below the water surface, with the mooring line from the buoy fastened to the weight. The mooring line was short enough so that the buoy would tow submerged. A sketch of this arrangement is shown in Figure 12.

To obtain the net drag of the buoys it was necessary to determine the tare drag of the supporting strut. This was done in two ways. The drag of the strut was first measured alone and then in the wake of the buoy in question. On both tests the strut was clamped to the towing beam of the drag dynamometer of the towing carriage, but in the latter test the buoy, supported independently of the towing strut by means of a U-frame, was maintained as close as possible to its original position relative to the strut without actually touching it; see Figure 13.

The tests of the  $\frac{1}{3}$ -scale models of Buoys 1 and 2 were limited to a maximum speed of 13 knots. The towing speed of Buoy 3 was limited to 9 knots because of excessive vibrations above that speed.

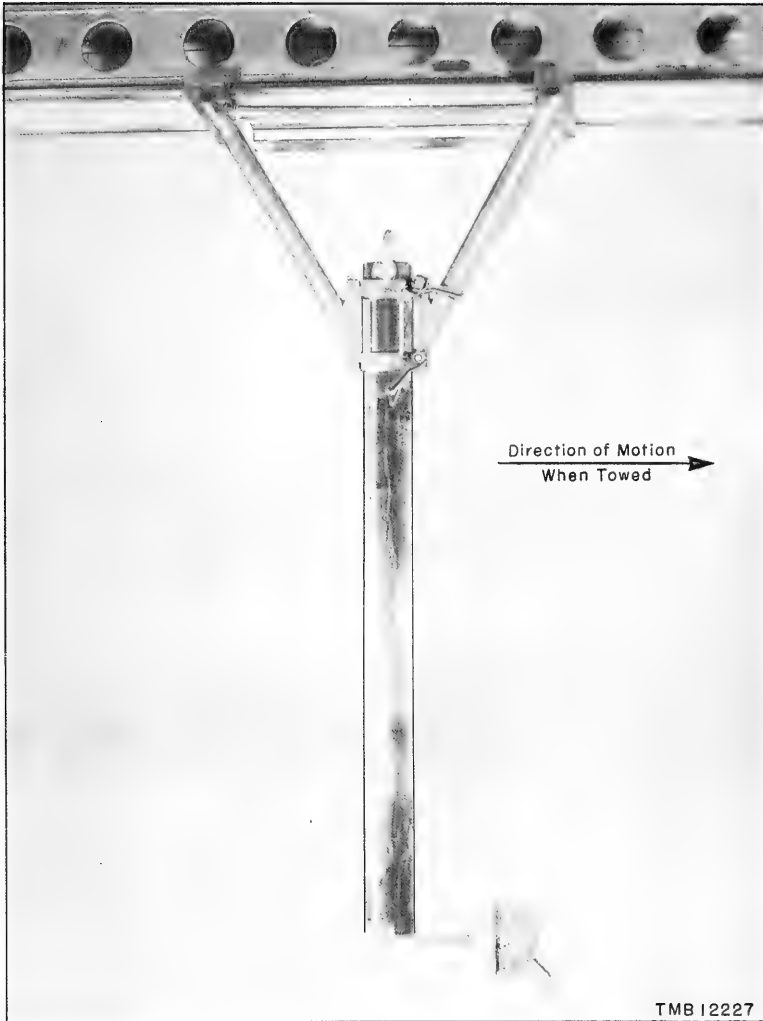


Figure 11 - General Towing Arrangement for Determining Drag of the Buoys

The 1/3-scale model of Buoy 2 is shown fastened to the end of the towing strut. The strut is clamped in a bracket fastened to the drag dynamometer beam of the towing carriage.

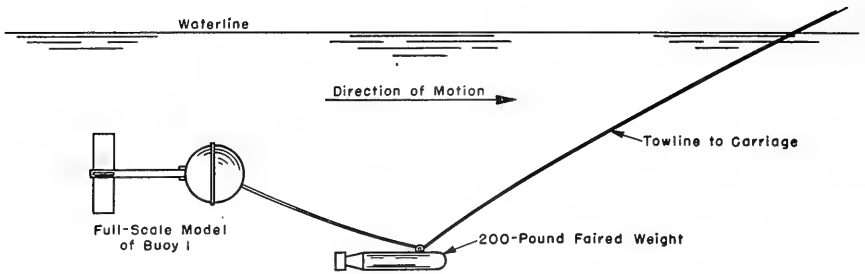


Figure 12 - Towing Arrangement for Stability Tests of Full-Scale Model of Buoy 1

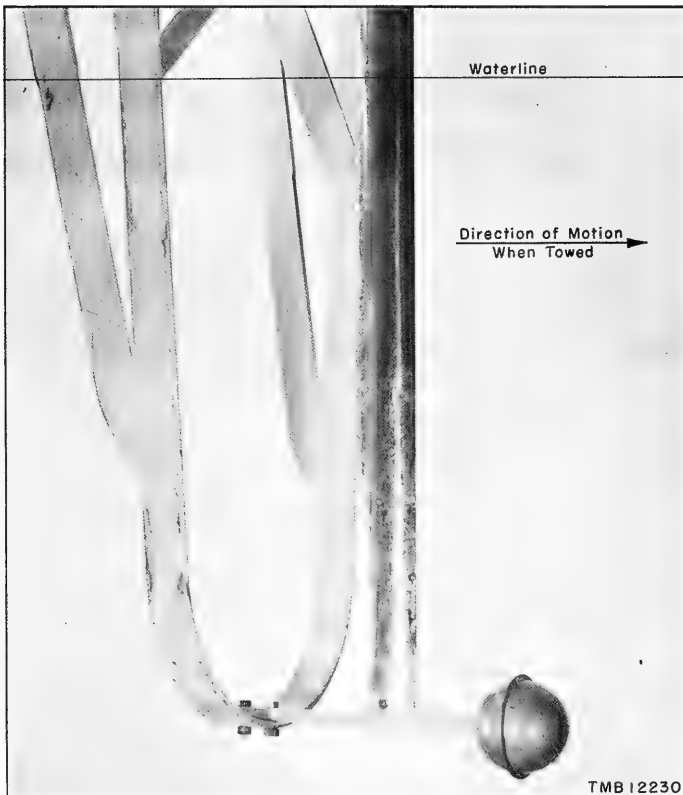


Figure 13 - Arrangement for Measuring the Tare Drag of the Towing Strut

The U-frame is used to support the buoy independently of the strut while the tare drag of the strut in the wake of the buoy is measured.

### TEST RESULTS

The pins inserted in Buoy 1 tend to increase the drag slightly, as can be seen in Figure 14.

The bail when fastened to Buoy 2 definitely increases the drag, as shown in Figure 15.

An interesting effect may be seen in regard to Buoy 3. At low speeds up to 5 1/2 knots the ball causes an increase in drag, but from 5 1/2 to 9 knots it leads to a decrease; see Figure 16.

The full-scale model of Buoy 1 with fins was towed for drag measurements; the results are presented in Figure 17.

The drag data obtained from tests on the full-scale model of Buoy 1 and the computed full-scale data as obtained from test data of the 1/3-scale model are compared in Figure 18. Drag data of the full-scale model of Buoy 1 include the drag of the fins.

During the stability tests of the full-scale model of Buoy 1, the buoy oscillated from side to side at the end of the towline in a plane normal to the direction of motion. As the speed increased, the period of oscillation decreased. There apparently was no pitching oscillation. It is interesting to note that the period of oscillation of the buoy is very nearly the same as that of a cylinder. The observed periods of lateral oscillation of the buoy are compared in Table 1 with the computed period of oscillation of a cylinder.

TABLE 1  
Oscillation of Buoy 1

| Speed Knots | Period of Buoy<br>Oscillation<br>seconds | Period of Cylinder<br>Oscillation<br>seconds |
|-------------|------------------------------------------|----------------------------------------------|
| 1.0         | 5.30                                     | 4.80                                         |
| 2.0         | 2.00                                     | 2.40                                         |
| 3.0         | 1.50                                     | 1.60                                         |
| 4.0         | 1.00                                     | 1.20                                         |
| 5.0         | 0.90                                     | 0.96                                         |

The period of lateral oscillation of the full-scale model of Buoy 1 when towed at the end of a short section of towline from an underwater towpoint is compared with computed values for a cylinder towed with its axis normal to the stream. If the same value for the Strouhals number is assumed for the buoy as for a cylinder of the same diameter, the period of oscillation of the cylinder can readily be computed. A free cylinder in a stream

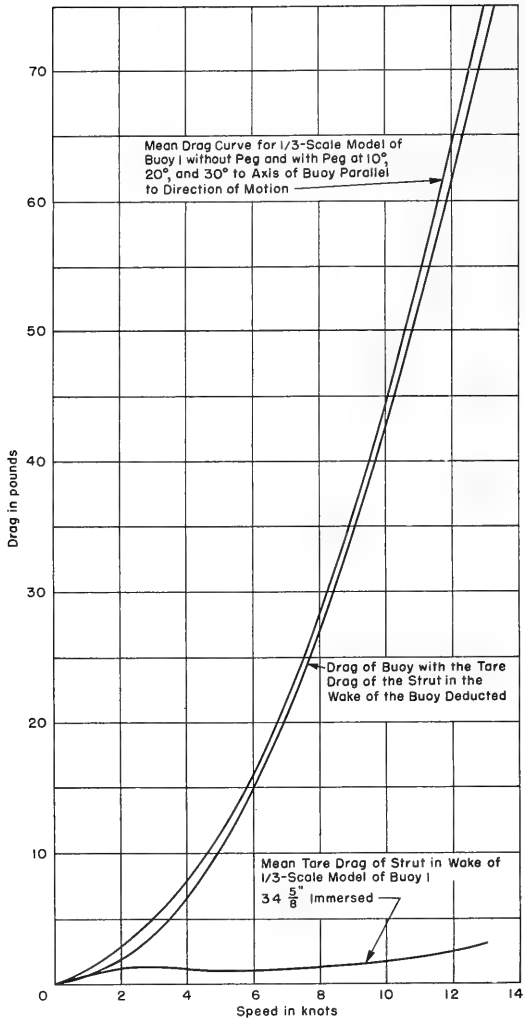


Figure 14 - Drag of 1/3-Scale Model of Buoy 1



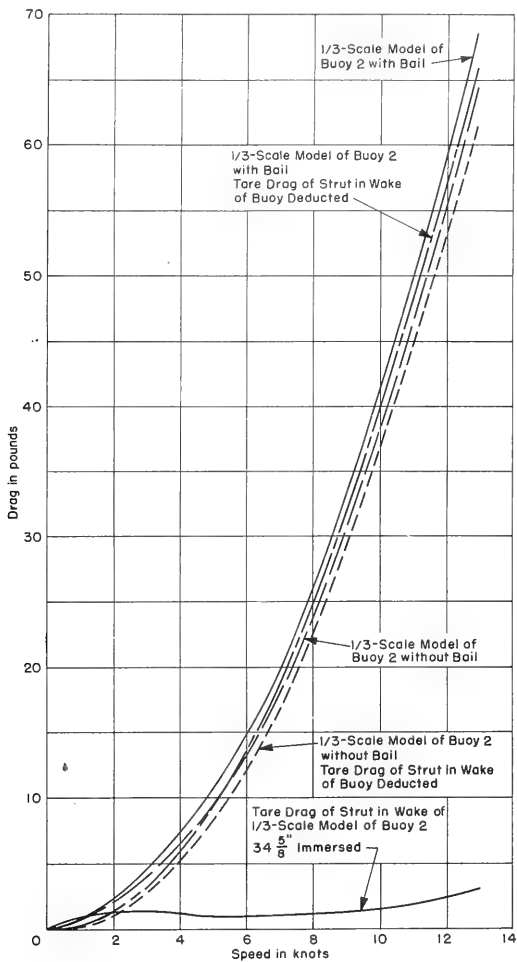


Figure 15 - Drag of 1/3-Scale Model of Buoy 2

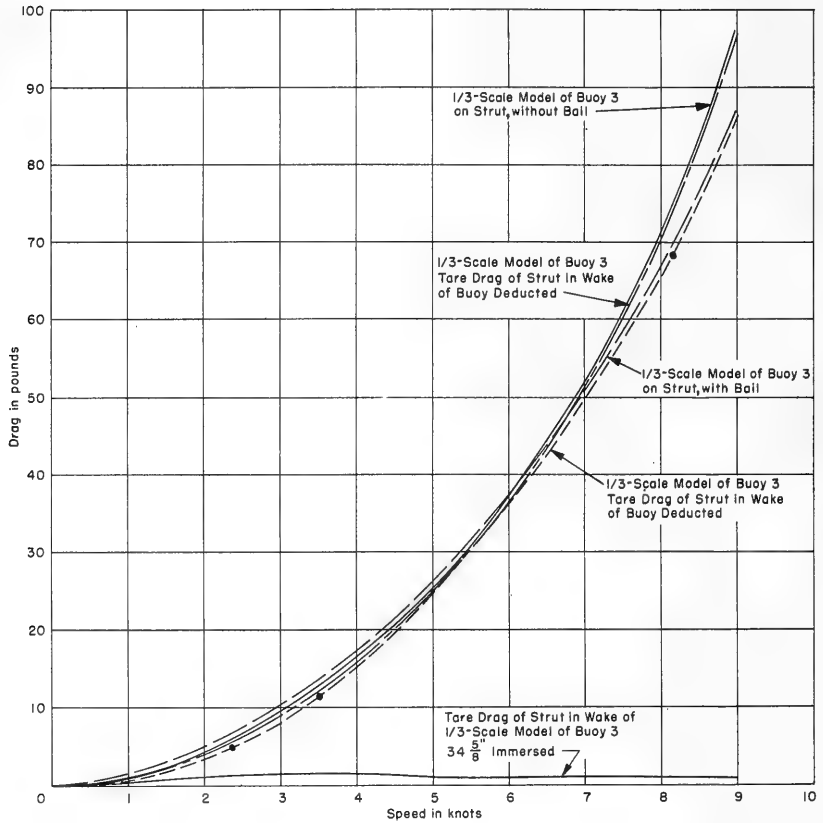


Figure 16 - Drag of 1/3-Scale Model of Buoy 3

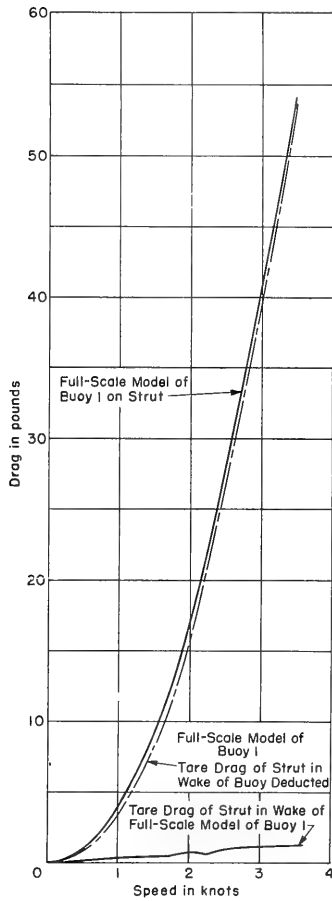


Figure 17 - Drag of Full-Scale Model of Buoy 1 with Fins

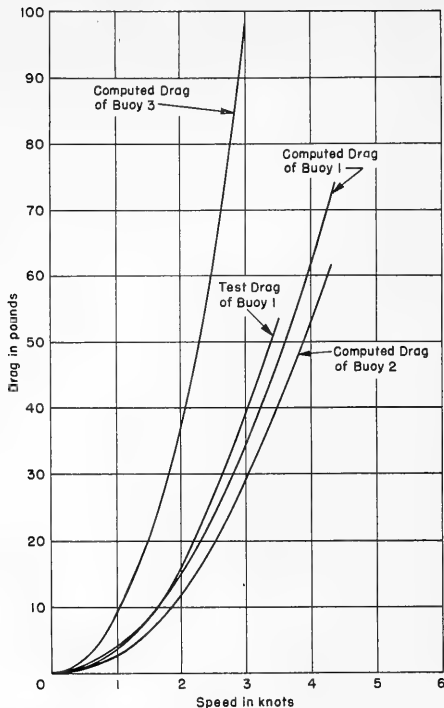


Figure 18 - Computed Full-Scale Drags of Buoys 1, 2, and 3 Compared with Experimental Full-Scale Drag of Buoy 1

flowing normal to the axis of the cylinder tends to oscillate with frequency  $n$  given by Strouhals number

$$\frac{nd}{V} = 0.185$$

where  $d$  is the diameter of the cylinder in feet and  $V$  is the velocity in feet per second (3)

#### TARE DRAG RESULTS

The tare drag of the strut, which was deducted from the total drag of the buoys and the strut combined, is the mean of the tare drag data obtained from tests on the strut when it was towed in the wake of the buoys. Figures 14 to 18 are curves in which the mean tare drag for the respective buoys is plotted against speed.

Figure 19 presents test data of the buoys in the form of a plot of drag coefficient versus Reynolds number. The drag coefficient is defined as

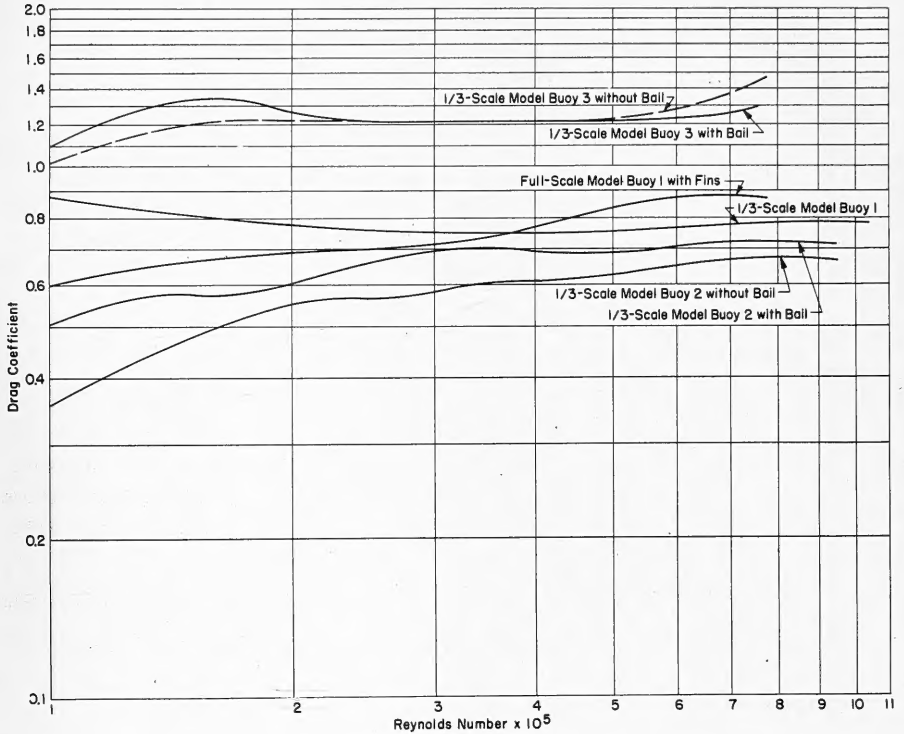


Figure 19 - Drag Coefficient Versus Reynolds Number for Various Buoy Models

$$C_D = \frac{D}{\frac{1}{2} \rho V^2 A}$$

where  $D$  is the drag of the buoy in pounds,

$\rho$  is the density of the water in slugs per cubic foot,

$A$  is the maximum projected area of the buoy into a plane normal to the flow, in square feet, and

$V$  is the towing speed in feet per second.

The Reynolds number is defined as

$$R = \frac{Vd}{\nu}$$

where  $V$  is the towing speed in feet per second,

$d$  is the maximum diameter of the buoy, and

$\nu$  is the kinematic viscosity in feet<sup>2</sup> per second.

CONCLUSIONS

From the analysis of the test data on Buoys 1, 2, and 3 it was possible to select that buoy which would meet the requirements established by the Woods Hole Oceanographic Institution (1).

The requirement that the drag coefficient remain fairly constant for a range of Reynolds numbers from  $1.0 \times 10^5$  to  $7.5 \times 10^5$  was satisfied by both Buoys 1 and 3; see Figure 19. The other requirement, that the buoy selected be reasonably stable in currents up to 5 knots, full-scale speed, was satisfied only by Buoy 1. The full-scale model of Buoy 1 was selected as the one most nearly fulfilling these requirements.

Buoy 1 will be further developed by the Woods Hole Oceanographic Institution.

REFERENCES

- (1) Conference at the David Taylor Model Basin 15 March 1944, between Dr. J.L. Hough and Mr. P. Osborn of the Woods Hole Oceanographic Institution and Messrs. L. Landweber, G. Grimminger, and R. A. Ebner of the Taylor Model Basin staff.
- (2) Equipment Information Booklet, David Taylor Model Basin, July 1942.
- (3) Goldstein, S., "Modern Developments in Fluid Dynamics," Vol. 2, p. 571, 1938.



